ENVIRONMENTAL
Science & Technology

November 3, 2020
Volume 54
Number 21
pubs.acs.org/est

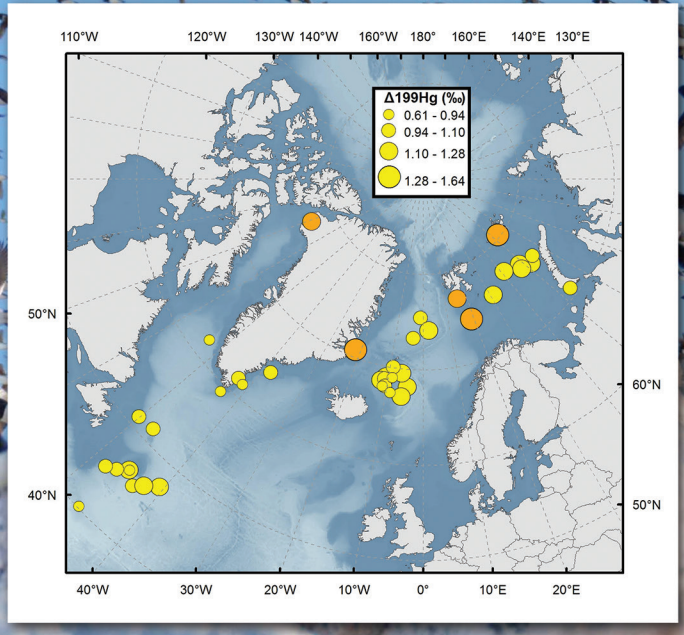

Methylmercury in the Arctic: Spatial and Isotopic Tracking using Seabirds

ACS Publications
Most Trusted. Most Cited. Most Read.

www.acs.org

Environmental Science & Technology

pubs.acs.org/est

Article

Contrasting Spatial and Seasonal Trends of Methylmercury Exposure Pathways of Arctic Seabirds: Combination of Large-Scale Tracking and Stable Isotopic Approaches

Marina Renedo,* David Amouroux, Céline Albert, Sylvain Bérail, Vegard S. Bråthen, Maria Gavrilo, David Grémillet, Hálfdán H. Helgason, Dariusz Jakubas, Anders Mosbech, Hallvard Strøm, Emmanuel Tessier, Katarzyna Wojczulanis-Jakubas, Paco Bustamante, and Jérôme Fort*

Cite This: https://dx.doi.org/10.1021/acs.est.0c03285

Read Online

ACCESS | Metrics & More | Article Recommendations | Supporting Information

ABSTRACT: Despite the limited direct anthropogenic mercury (Hg) inputs in the circumpolar Arctic, elevated concentrations of methylmercury (MeHg) are accumulated in Arctic marine biota. However, the MeHg production and bioaccumulation pathways in these ecosystems have not been completely unraveled. We measured Hg concentrations and stable isotope ratios of Hg, carbon, and nitrogen in the feathers and blood of geolocator-tracked little auk *Alle alle* from five Arctic breeding colonies. The wide-range spatial mobility and tissue-specific Hg integration times of this planktivorous seabird allowed the exploration of their spatial (wintering quarters/breeding grounds) and seasonal (nonbreeding/breeding periods) MeHg exposures. An east-to-west increase of head feather Hg concentrations (1.74−3.48 $\mu g \cdot g^{-1}$) was accompanied by significant spatial trends of Hg isotope (particularly Δ^{199}Hg: 0.96−1.13‰) and carbon isotope (δ^{13}C: −20.6 to −19.4‰) ratios. These trends suggest a distinct mixing/proportion of MeHg sources between western North Atlantic and eastern Arctic regions. Higher Δ^{199}Hg values (+0.4‰) in northern colonies indicate an accumulation of more photochemically impacted MeHg, supporting shallow MeHg production and bioaccumulation in high Arctic waters. The combination of seabird tissue isotopic analysis and spatial tracking helps in tracing the MeHg sources at various spatio-temporal scales.

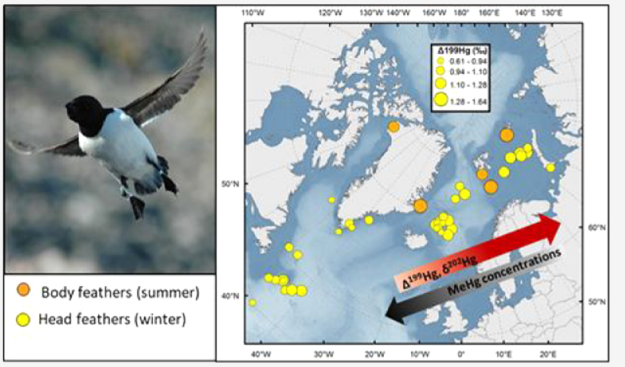

1. INTRODUCTION

Mercury (Hg) poses major risks for wildlife and human health, especially in its methylated form (methylmercury, MeHg), a potent bioaccumulative neurotoxin,[1] which is mainly assimilated via fish and seafood consumption. In the ocean, MeHg production mainly occurs by biotic in situ methylation of inorganic Hg.[2,3] Once formed, MeHg incorporates into the food webs and biomagnifies its concentrations, leading to life-impacting levels in top predators and humans. Despite little direct anthropogenic pressure in the Arctic region, Arctic ecosystems are subject to contamination by Hg transported from lower latitudes. Indeed, total Hg concentrations measured in the Arctic surface seawater are up to twofold higher compared to other oceanic regions.[4,5] Sea-ice melting, direct atmospheric deposition, and continental inputs originating from soil erosion and riverine circulation are considered major drivers of the high Hg levels in the Arctic.[6−10] However, the MeHg production pathways and zones in the Arctic Ocean have still not been completely identified. Several studies demonstrated that Hg in Arctic marine environments may be methylated in the water column or sediments.[2,11] Potential Hg-methylating bacteria were also identified in Antarctic sea-ice.[12] Recent findings and modeling studies evidenced that the largest net MeHg production in Arctic water columns may occur in oxic waters at the subsurface layer (20−200 m).[6,13] A new study also reported the high abundance of Hg-methylating genes in the oxic subsurface waters of the global ocean,[14] where the highest MeHg concentrations are typically observed.[4] All of these findings suggest that Hg methylation in oxic waters could be a significant source of MeHg toward Arctic marine food webs. Although policy implementations for the reduction of anthropogenic Hg emissions were achieved over the last 30 years in some parts of the world, Hg levels continue to increase in biota from several regions of the Arctic.[15] Medium to high predators such as seabirds are

Received: May 22, 2020
Revised: September 30, 2020
Accepted: October 1, 2020

exposed to significant environmental MeHg concentrations through their diet[15,16] and have been extensively studied as bioindicators of Hg exposure in marine food webs (e.g[17,18]), including the Arctic.[19−21] Specific foraging habitats and migratory movements of Arctic seabirds strongly determine their exposure to distinct environmental MeHg sources in marine ecosystems.[22,23] However, studies on Hg exposure in Arctic seabirds have commonly focused on the breeding season (summer), when seabirds are more accessible for researchers. Consequently, investigation of Hg exposure during the nonbreeding season is still scarce due to sampling logistical difficulties.

The combination of carbon and nitrogen stable isotopes with Hg stable isotopes has demonstrated its suitability for the identification of Hg sources and the associated geochemical processes in the different marine compartments.[24−26] Therefore, its use can help toward understanding Hg exposure pathways of seabirds according to their migratory behavior. Hg has seven stable isotopes (196−204) and fractionates with and without dependence on the isotopic masses. The combined use of Hg isotopic mass-dependent (MDF, e.g., δ^{202}Hg) and mass-independent (MIF, e.g., Δ^{199}Hg) fractionation enables the quantification of processes and the identification of sources and pathways of Hg in the environment,[27] including marine ecosystems.[25,26,28,29] MDF of Hg isotopes occurs during many physical, chemical, or biological processes.[30−33] However, large Hg MIF of odd isotopes (Δ^{199}Hg and Δ^{201}Hg) is observed during light-induced reactions, such as inorganic Hg photoreduction and MeHg photodemethylation. Hg MIF signature is not affected by biological or trophic processes, so it is preserved up to the food webs,[34] thus presenting a significant advantage to trace Hg marine sources. For instance, Arctic marine top predators had much higher Hg odd-MIF values (more photochemically impacted Hg) in non-ice-covered regions, indicating the importance of the accelerated melting of sea-ice in the Hg polar cycle.[25,35] Also, a consistent decrease of Hg odd-MIF (and MDF) in pelagic fish according to their foraging depth in the North Pacific Ocean demonstrated the dilution of surface MeHg by in situ methylated Hg at depth.[3] More recently discovered MIF of even Hg isotopes (reported as Δ^{200}Hg) seems to occur during complex atmospheric mechanisms such as photo-oxidation in the tropopause.[36] Even MIF is not induced during any biogeochemical or photochemical processes in the lower troposphere or the photic zone;[36−38] therefore, the signature is preserved and useful to identify major potential Hg sources of atmospheric origin.[10,39,40] Due to the different combinations of the processes involving Hg transformations in the environment, Hg isotopes fractionate differently and with different degrees of magnitude in every specific environmental compartment. Thus, the analysis of Hg stable isotopes of mobile predators such as Arctic seabirds can provide interesting information about MeHg trophic sources at large scales of the Arctic Ocean and neighboring water bodies.

Here, we propose an original approach consisting of the combination of isotopic analyses (Hg, C, and N) and wildlife tracking to provide new information about MeHg exposure pathways of seabirds at both temporal and spatial scales. For this purpose, we focused on the little auk (or dovekie, *Alle alle*), the most numerous seabird species breeding in the high Arctic (between 37 and 40 million breeding pairs estimated[41,42]). Little auks have several ecological advantages for their use as bioindicator models. (1) They are zooplanktivorous and mainly feed on copepods belonging to two *Calanus* species (i.e., *Calanus glacialis* and *Calanus hyperboreus*) during the breeding period.[43] Therefore, they reflect MeHg accumulation in a short food chain that is strongly dependent on sea-ice abundance and seawater temperature.[44] (2) They exhibit colony-specific wintering areas,[45] reflecting wide-ranging spatial variability of Hg exposure.[46] (3) Little auks molt their feathers twice during their annual cycle: a partial molt (head, neck, and throat feathers, hereafter "head feathers") during the prebreeding period (in ca. April) and a complete postbreeding molt in September.[13] During molt, seabirds excrete the Hg accumulated in their body tissues into the feathers.[47] Thus, feather Hg reflects blood Hg levels at the time of feather growth that occurred at the last molting sequence,[48] thus integrating Hg from the current diet and/or the remobilization of Hg from tissues during molt. Therefore, the different Hg integration times between the types of feathers allow us to study Hg exposure during both the nonbreeding (head feathers) and the breeding (body feathers) periods in the same individual.[46] Besides, C and N isotopic ratios of blood sampled during the breeding—chick-rearing—period can provide information about summer diet and then be compared to the Hg levels and isotopic composition in the body feathers of little auks.[49,50] We hypothesized that variations of tissue-specific Hg isotopic signatures (body vs head feathers) will allow reflecting the seasonal variability (summer vs winter) on the Hg cycling. Besides, the exploration of both spatial grounds and isotopic information (Hg, C, and N) would help in tracking distinct sources of Hg contamination along with seabird migratory circulation.

2. MATERIAL AND METHODS

2.1. Sampling Sites and Description of Sample Collection. This study was conducted during the seabird breeding seasons of 2015 and 2016 at five colonies of the Arctic Ocean: Franz Josef Land (FJL) (Hooker Island; 80.23°N, 53.01°E), Bear Island (Bjørnøya; 74.45°N, 19.04°E), East Greenland (Kap Høegh; 70.72°N, 21.55°W), Spitsbergen (Hornsund; 76.97°N, 15.78°E), and North West Greenland (Thule; 77.47°N, 69.22°W). Blood and feathers were sampled from 10 individuals per colony (n = 50 for the five colonies). Individuals from all sites, except Thule, were equipped with a miniature geolocator data-logger (GLS, Biotrack MK4083 or Migrate Technology C65) to track their nonbreeding movements and distribution, as described in previous works.[45,51,52] We treated GLS tracking data from December 1 to January 30 (the period when all little auks were at their winter grounds) and calculated the median individual winter latitude and longitude for each individual separately.

2.2. Description of Analytical Methods. *2.2.1. Sample Preparation, Analyses of Total Hg and Hg Species Concentrations.* Body and head feathers were cleaned in a 2:1 chloroform/methanol solution for 5 min in an ultrasonic bath, followed by two methanol rinses to remove surface impurities, and then oven-dried at 50 °C for 48 h and homogenized to powder.[46] Since fluctuations of Hg concentrations have been observed among and within individual feathers from the same bird,[53,54] we pooled a representative number of feathers of each individual (5−8 feathers) to limit the variability and provide results as accurately as possible. Blood samples were dried, lyophilized, and ground to powder as described in previous work.[46] Feather and blood total Hg concentrations (hereafter expressed as $\mu g \cdot g^{-1}$, dry weight)

https://dx.doi.org/10.1021/acs.est.0c03285
Environ. Sci. Technol. XXXX, XXX, XXX−XXX

were quantified using an advanced Hg analyzer (AMA-254, Altec).

Prior to Hg speciation analyses, blood and feathers (0.01−0.05 g) were digested following a previously developed method by microwave-assisted extraction (using a Discover SP-D microwave, CEM Corporation).[55,56] We used 5 mL of tetramethylammonium hydroxide (25% TMAH in H_2O, Sigma-Aldrich) for blood samples and 5 mL of nitric acid (HNO_3·6N, Instra quality) for feather Hg extraction. The extraction was carried out in CEM Pyrex vessels by 1 min of warming up to 75 °C and 3 min at 75 °C with magnetic agitation to homogenize the samples. Quantification of Hg species was carried out by isotope dilution analysis (details in ref 55), using a GC-ICP-MS Trace Ultra GC equipped with a TriPlus RSH autosampler coupled to an ICP-MS XSeries II (Thermo Scientific). We performed Hg speciation analyses of certified reference materials (CRM) for QA/QC purposes (Table S1). Human hair reference material (NIES-13) and feather internal reference material (F-KP, king penguin feathers) were used for validation of feather analyses (keratin-based matrixes). Blood analyses were validated with dogfish liver reference material (DOLT-5) and with internal reference material (RBC-KP, king penguins red blood cells). The reported results of the total Hg concentrations obtained by Hg speciation analyses (i.e., the sum of inorganic and organic Hg) were compared to the total Hg concentrations obtained by AMA-254 to verify the recovery of the extraction. Recoveries of Hg and MeHg concentrations with respect to the reference values for each material varied between 92 and 108% (Table S1).

2.2.2. Total Hg Isotope Analyses. Feather (and blood) samples (0.05−0.10 g) were digested with 3 or 5 mL of HNO_3 acid (65%, Instra quality) after a predigestion step overnight at room temperature. Hg extraction was carried out by Hotblock heating at 75 °C for 8 h (6 h in HNO_3 and 2 h more after addition of 1/3 of the total volume of H_2O_2 30%, ULTREX quality). The digested mixtures were finally diluted in an acidic matrix (10% HNO_3 and 2% HCl), with the final Hg concentrations ranging from 0.5 to 1 ng·mL^{-1}. Hg isotopic composition was determined using a cold-vapor generator (CVG)-multiple-collector inductively coupled plasma mass spectrometer (MC-ICP-MS) (Nu Instruments), as detailed in previous work.[56] Hg isotopic values were reported as δ notation, calculated relative to the bracketing standard NIST SRM-3133 reference material to allow interlaboratory comparisons, as described in the Supporting Information. NIST SRM-997 thallium standard solution was used for the instrumental mass-bias correction using the exponential law. Secondary standard NIST RM-8160 (previously UM-Almadén standard) was used for validation of the analytical session (Table S2).

Recoveries of extraction were verified for all samples by checking the signal intensity obtained on the MC-ICP-MS for diluted extracts relative to the NIST 3133 standard (with an approximate uncertainty of ±15%). Total Hg concentrations in the extract solution were compared to the concentrations found by AMA-254 analyses to assess method recovery. Total Hg concentrations in the extract solution were compared to the concentrations found by AMA-254 analyses to assess method recovery. Average recoveries obtained were 98 ± 14% for feathers (n = 104) and 100 ± 2% for blood samples (n = 102). The accuracy of Hg isotopic analyses for keratin matrixes was evaluated with validated human hair material NIES-13 isotopic composition.[57] Hg isotopic results for blood samples were validated with reference values of Lake Michigan fish tissue NIST SRM 1947. Internal reference samples of feathers (F-KP) and avian blood (RBC-KP) were also measured. Uncertainty for δ values was calculated using 2SD typical errors for each internal reference material (Table S2).

2.2.3. Carbon and Nitrogen Stable Isotope Analyses. Homogenized feather and blood subsamples (aliquots mass: ∼0.3 mg) were weighed with a microbalance and packed in tin containers. Carbon ($\delta^{13}C$) and nitrogen ($\delta^{15}N$) stable isotope ratios were determined with a continuous flow mass spectrometer (Thermo Scientific Delta V Advantage) coupled to an elemental analyzer (Thermo Scientific Flash EA 1112). Results are in δ notation relative to Vienna PeeDee Belemnite and atmospheric N_2 for $\delta^{13}C$ and $\delta^{15}N$, respectively. Replicate measurements of internal laboratory standards (acetanilide) indicated measurement errors <0.15‰ for both $\delta^{13}C$ and $\delta^{15}N$ values. USGS-61 and USGS-62 reference materials were also analyzed for calibration.

2.3. Statistical Analyses. Statistical analyses were performed using the software R 3.3.2 (R Core Team, 2018).[58] Before statistical analyses, the data were checked for normality of distribution and homogeneity of variances using Shapiro−Wilk and Breusch−Pagan tests, respectively. Since data did not meet the specificities of normality and homoscedasticity, nonparametrical tests (Kruskal−Wallis with Conover−Iman post hoc test) were performed. Statistically significant results were set at α = 0.05. Statistical significance of Hg concentration and isotopic differences between head and body feathers were assessed using a randomization procedure. A 99% confidence interval was calculated by means of the bootstrap estimation method (n = 1000 iterations).

We examined the correlations between Hg concentrations, $\delta^{13}C$, Hg MDF ($\delta^{202}Hg$) and MIF ($\Delta^{199}Hg$ and $\Delta^{200}Hg$), latitude, and longitude using linear regressions and Spearman correlation rank tests. The influence of the latitude and longitude of their individual breeding and nonbreeding distributions on feather Hg isotopic signatures was tested using linear mixed models (LMMs) with colonies as the random effect in the whole data set, using the R package "lme4".[59] Summer latitude, summer longitude, and both summer latitude + longitude together were used as predictors for Hg isotopic signatures of body feathers. Similarly, median winter latitude, median winter longitude, and both medians together were used as predictors of Hg isotopic signatures in head feathers. Variance inflation factors were always <3,[60] ensuring that there was no collinearity between latitude and longitude in summer (breeding colonies) and median latitude and longitude in winter (wintering areas).[61] The different models were ranked based on Akaike's information criteria (AICc) adjusted for small sample sizes and compared using ΔAICc and Akaike weights (w) using the R package "wiqid".[62] To assess the explanative power of these models, marginal R^2 was obtained using the R package "r2glmm".[63]

3. RESULTS AND DISCUSSION

3.1. Seasonal and Geographical Variations of Feather MeHg Concentrations Related to Changing Foraging Habits ($\delta^{15}N$). We observed that the dominant fraction of Hg was in the form of MeHg both in body feathers and in blood (94 ± 2%, n = 20, and 90 ± 3%, n = 10, respectively) for all of the studied populations of little auks (Table S3). This result is in good agreement with previous studies[55,56,64,65] and supports the fact that both tissues of little auks principally present Hg as

https://dx.doi.org/10.1021/acs.est.0c03285
Environ. Sci. Technol. XXXX, XXX, XXX−XXX

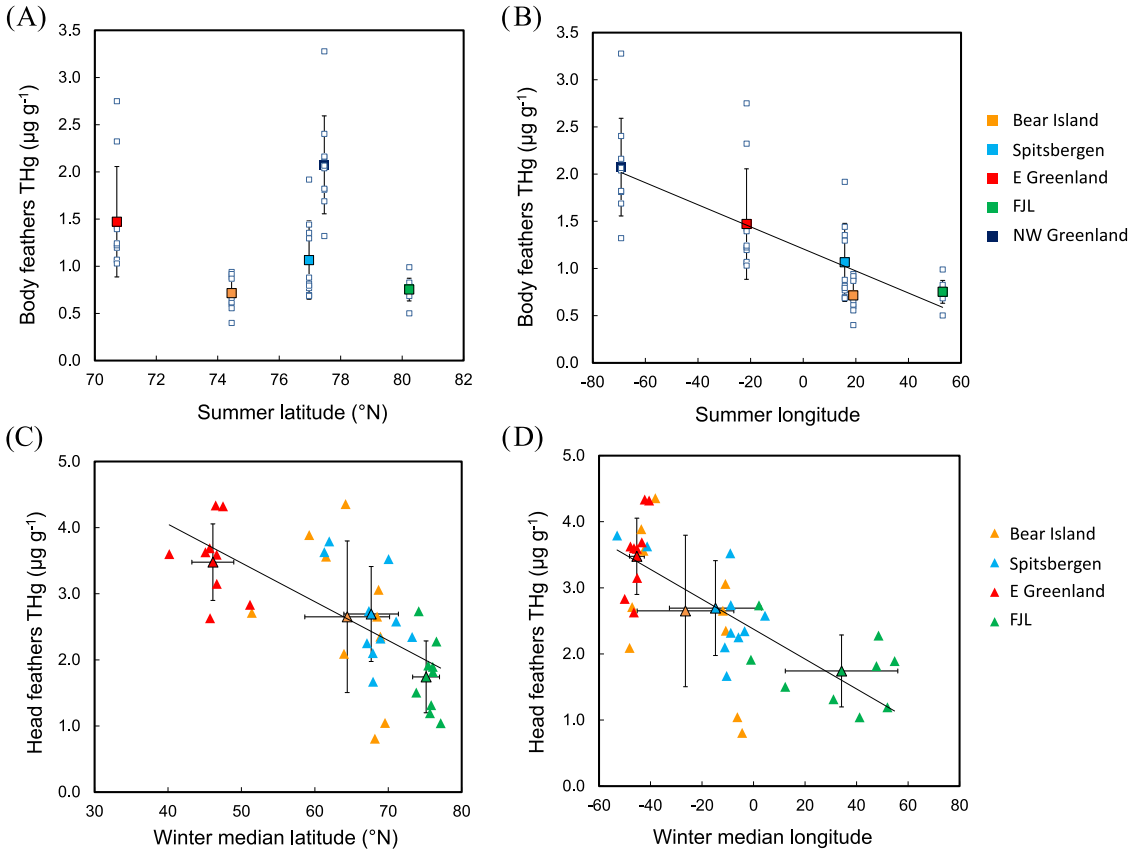

Figure 1. Total Hg concentration ($\mu g \cdot g^{-1}$) of little auk body feathers (summer) as a function of the (A) latitude and (B) longitude of their breeding sites and head feathers (winter) as a function of the (C) median latitude and (D) median longitude of their winter grounds. Regression lines are (A) slope: 0.052 ± 0.013, intercept: −3.420 ± 0.997, R^2 = 0.26, p = 0.005; (B) slope: −0.012 ± 0.001, intercept: 1.209 ± 0.059, R^2 = 0.58, p < 0.0001; (C) slope: −0.059 ± 0.011, intercept: 6.399 ± 0.669, R^2 = 0.54, p < 0.0001; and (D) slope: −0.022 ± 0.003, intercept: 2.375 ± 0.120, R^2 = 0.60, p < 0.0001. Regression lines are presented only for significant relationships between the two variables.

MeHg. Body and head feathers are known to grow at different times and therefore the Hg excreted in head and body feathers reflects, respectively, the exposure during their wintering (October to April) and breeding (May to September) periods. Since birds are known to excrete between 70 and 90% of their Hg body burden by feather molt,[48] we cannot exclude that some residual Hg accumulated during the nonbreeding period could also be excreted during body feather molt, and vice versa, but this fraction would be minor.

Overall, individuals presented higher Hg (MeHg) concentrations in head compared to body feathers, exhibiting up to twofold higher concentrations in head feathers in the case of East Greenland and Bear Island populations (Table S4). Higher Hg concentrations of head feathers are in agreement with previous observations[22] and suggest higher exposure to MeHg during the nonbreeding period outside the High Arctic. For instance, little auks breeding in areas of Spitsbergen and East Greenland are known to mainly forage on copepods (*Calanus* spp.) during the breeding season.[43] However, the seasonal vertical migration of their main prey *Calanus* spp. to inaccessible depths produces a seasonal shift in their diet toward krill *Meganyctiphanes norvegica*, Hyperiid Amphipods *Themisto* spp., and fish larvae.[66] The consumption of higher trophic level prey during winter could explain the higher Hg levels excreted during the spring molt (head feathers), whereas they are probably less exposed to Hg in summer.

We also observed high variations of Hg concentrations in head feathers among individuals of the same colony, especially in Bear Island (from 0.81 to 4.35 $\mu g \cdot g^{-1}$) and Spitsbergen populations (from 1.67 to 3.79 $\mu g \cdot g^{-1}$) (Figure S1). This could be due to the widespread individual foraging specialization during their nonbreeding period and the consumption of a wider range of prey.[67] Conversely, little auks occupy more restricted foraging areas during the breeding season due to the need to frequently feed their chicks and therefore feed on local prey captured near their respective colonies,[68] leading to less intrapopulation variability of Hg concentrations in their body feathers.

We observed a consistent longitudinal trend of body feather Hg concentrations (R^2 = 0.58, p < 0.0001) with increasing Hg levels from eastern (Bear Island and FJL, 0.71 and 0.75 $\mu g \cdot g^{-1}$, respectively) to western colonies (NW Greenland, 2.07 $\mu g \cdot g^{-1}$) (Figure 1). When applying mixed models, summer longitude was the most supported predictor of body feather Hg concentrations (Table S6). Head feather Hg concentrations were positively correlated both with winter latitude and longitude for the four spatially tracked populations (R^2 = 0.54 and 0.60, respectively, both p < 0.0001) (Figure 1). Both variables together were considered as predictors of Hg head feather concentrations by linear mixed models (Table S7). Head feather concentrations were higher in populations wintering in western zones (3.48 $\mu g \cdot g^{-1}$, East Greenland population) and decreased gradually and significantly (H = 20.13, p = 0.001) in those wintering in northeast areas (1.74 $\mu g \cdot g^{-1}$, FJL population). The consistent longitudinal patterns both in summer and winter reflect a higher accumulation of

https://dx.doi.org/10.1021/acs.est.0c03285
Environ. Sci. Technol. XXXX, XXX, XXX−XXX

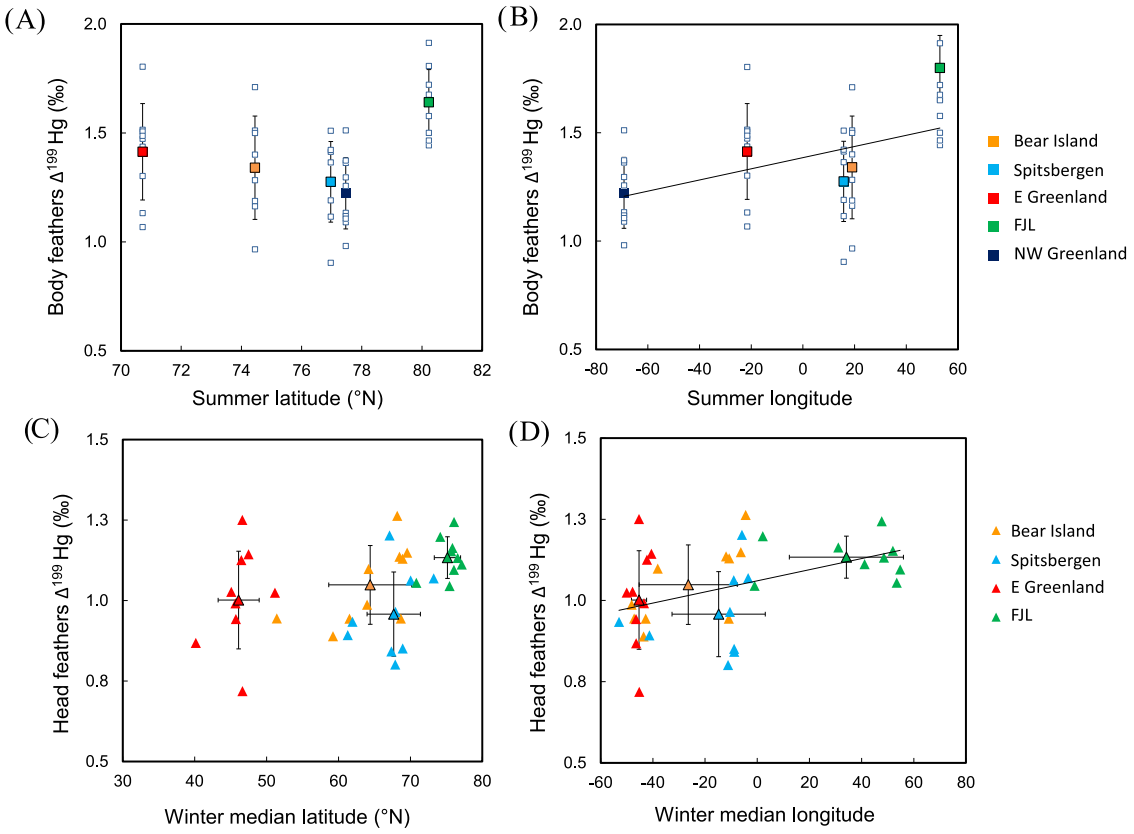

Figure 2. Hg odd-MIF (Δ^{199}Hg) of little auk body feathers (summer) as a function of (A) latitude and (B) longitude of their breeding sites and head feathers (winter) as a function of the (C) median latitude and (D) median longitude of their wintering grounds. Regression lines are (A) slope: 0.014 ± 0.011, intercept: 0.319 ± 0.822; R^2 = 0.01, p = 0.20; (B) slope: 0.002 ± 0.001, intercept: 1.384 ± 0.031, R^2 = 0.20, p < 0.0001; (C) slope: 0.004 ± 0.002, intercept: 0.784 ± 0.123, R^2 = 0.07, p = 0.06; and (D) slope: 0.001 ± 0.001, intercept: 1.069 ± 0.022, R^2 = 0.22, p = 0.002. Regression lines are presented only for significant relationships between the two variables.

MeHg in little auks from western regions, whereas colonies breeding in Arctic northern regions seem to be exposed to lower concentrations.

Seabird blood δ^{15}N values provide short- to medium-term information (about 1−5 weeks), while feather δ^{15}N values reflect the diet at the time they were grown.[50,69] The distribution of little auk populations in winter was limited to the North Atlantic and the Arctic areas, where large-scale δ^{15}N values are known to be relatively homogeneous at the base of the food web,[70,71] thus allowing the interpopulation comparison. The lower body feather Hg concentrations and blood δ^{15}N values observed in little auks (Table S5) suggest that all birds from the different populations mostly feed at low trophic levels and on *Calanus* copepods in summer. In contrast, the interpopulation differences of the δ^{15}N values in winter (head feathers) were much more pronounced (Table S4). For instance, little auk populations breeding in FJL and Bear Island exhibited ∼3‰ higher δ^{15}N values in head feathers than in blood. This difference highlights the spatial variability of δ^{15}N values in relation to the different winter distribution of little auks in winter. Previous studies have reported significant seasonal variations in copepod δ^{15}N values (up to 6‰) between late winter and spring (highly productive periods) relative to the summer and autumn periods.[71,72] The seasonal variability of zooplankton δ^{15}N values is common in the eastern and western parts of the North Atlantic Ocean and needs to be considered here due to the wide spatial distribution of little auks in winter. Therefore, the higher feather Hg concentrations of little auk colonies from western parts of the Arctic Ocean could be influenced by their seasonal dietary shifts and different spatial distribution but also by the complex Hg oceanic dynamics or distinct environmental sources that control the level of exposure to MeHg at the different regions.

3.2. Spatio-Temporal Trends of Hg MDF (δ^{202}Hg) in Feathers Related to Ecological Aspects. Specific Hg integration times of seabird tissues may influence the seasonal incorporation of MeHg from different spatial origins.[73] However, the geographical variations in δ^{202}Hg values are generally difficult to distinguish since metabolic processes also induce Hg MDF. Head and body feathers showed large ranges of δ^{202}Hg values, varying from −0.24 to 1.43‰ and from −0.11 to 1.28‰, respectively. Although we focused on the study of multiple colonies of the same seabird species to minimize the metabolic or trophic-related effects, we cannot exclude that the variability of δ^{202}Hg signatures among colonies is led only by the specific isotopic baseline of their respective foraging habitats. For instance, the FJL population exhibited significantly higher δ^{202}Hg values relative to the other four populations, both in head (H = 29.42, p < 0.0001) and body feathers (H = 27.69, p < 0.0001) (Table S4). It is known that little auks from FJL are morphologically bigger than those of the populations from Svalbard due to more severe climate conditions in this area.[74] Thus, potentially different morphological characteristics associated with their bigger size could contribute to higher feather δ^{202}Hg values in this colony. Hg

https://dx.doi.org/10.1021/acs.est.0c03285
Environ. Sci. Technol. XXXX, XXX, XXX−XXX

concentrations and δ^{202}Hg values of head feathers were highly correlated for the overall populations (R^2 = 0.52, p < 0.0001), while Δ^{199}Hg signatures were not related to Hg concentration in any type of feather (Figure S2). This observation shows the completely decoupled behavior between δ^{202}Hg and Δ^{199}Hg signatures. The influence of biological and ecological factors on δ^{202}Hg values shows the limitation of this type of signature in discerning spatial MeHg sources related to different migratory routes of seabird populations. The utilization of feather δ^{202}Hg values as a proxy of geographical patterns or to changing environmental conditions requires complete knowledge of all of the processes and factors driving Hg MDF (i.e., trophic ecology and intrinsic metabolic/physiological processes).

3.3. Hg Odd-MIF (Δ^{199}Hg): Seasonal and Spatial Differences of Hg Marine Photochemistry. Head and body feather odd-MIF values (Δ^{199}Hg) ranged from 0.72 to 1.26‰ and 0.90 to 1.91‰, respectively. Significantly higher Δ^{199}Hg values in body compared to head feathers (Table S8) suggest a seasonal variability in odd-MIF values. This could be primarily associated with the vertical migration of little auk main prey (copepods) and the consequent seasonal shift in their diet to krill/amphipods during the winter season. Their seasonal diet shift could enhance the accumulation of pelagic MeHg that is less connected to the photic zone during winter, thus leading to lower Δ^{199}Hg values of the MeHg excreted into head feathers. A previous study on sub-Antarctic penguins documented significant differences of Δ^{199}Hg values as a function of their specific foraging depths,[24] increasing around 0.4‰ from benthic to epipelagic populations. Although the little auk populations studied here are known to mainly feed on the same prey items and forage at similar depths, we should consider that changes in the availability of their prey among sites could also contribute to different feather Δ^{199}Hg values among populations. Further, due to the diurnal migration of zooplankton from deep water to the surface, the mixed pool of Hg accumulated in these organisms originates from different depths of the water column and, therefore, their Δ^{199}Hg values represent a mixture of deep (low photodemethylated) Hg and surface Hg uptake.[75] Together with the trophic and ecological factors, we could expect that the seasonal variability of feather Δ^{199}Hg values (body vs head feathers) of little auks could be also influenced by a higher extent of Hg marine photochemistry occurring during summer. In springtime/summer, little auks are known to return to their breeding sites, located at northern latitudes, where they are exposed to longer daily photoperiods at this time of the year (polar day). Nevertheless, the small differences of Δ^{199}Hg values between body and head feathers of the same population (from 0.26 to 0.50‰, Table S8) seem to indicate low variations of MeHg photodemethylation extents between their summer and winter sites. Therefore, the differences in the daily photoperiod and/or light penetration between their summer and wintering foraging grounds would play a minor role in Hg isotopic variations.

Concerning the spatial variability of Δ^{199}Hg values among colonies, we observed positive linear relationships between body feather Δ^{199}Hg values and summer longitude (R^2 = 0.20, p < 0.0001) and between head feather Δ^{199}Hg values and winter longitude (R^2 = 0.22, p < 0.0001) (Figure 2). Summer and winter longitudes were, respectively, the most supported explanatory factors of body and head feather Δ^{199}Hg values (Tables S6 and S7). No significant relationships were observed with latitude in summer (R^2 = 0.01, p = 0.20) or winter (R^2 = 0.07, p = 0.06) (Figure 2). The FJL population, the northern colony of this study, showed slightly higher body feather Δ^{199}Hg values (1.64 ± 0.15‰, n = 10, 80°N) compared to other studied colonies (1.31 ± 0.20‰, n = 37 70−77°N) (H = 11.96, p = 0.018). FJL individuals also presented higher Δ^{199}Hg values in their head feathers (1.13 ± 0.06‰) compared to the other colonies (1.00 ± 0.12‰) (H = 18.55, p = 0.001). Previous studies on Alaskan seabirds reported around twofold higher mean Δ^{199}Hg signatures in low-ice-covered oceanic areas (1.13 ± 0.16‰; 56−58°N) than highly ice-covered regions (0.53 ± 0.15‰; 68°N) and revealed that the presence of sea-ice inhibits light penetration and, therefore, Hg marine photochemistry.[25] Compared to the latitudinal trend observed in Alaska, the spatial variations of Δ^{199}Hg values between northern and southern populations of little auks are relatively small and, interestingly, presented an inversed tendency between highly ice-covered (FJL) and non-ice-covered areas (North Atlantic regions). Therefore, we cannot presume that the presence of sea-ice is a driving factor controlling MeHg photochemistry and the related odd-MIF signatures registered in the feathers of little auks. The existence of an opposed latitudinal trend of Δ^{199}Hg values between the eastern and western Arctic Ocean regions reveals different Hg dynamic systems, especially for Hg accumulation pathways in food webs.

According to previous findings, the largest MeHg production in the Arctic water column seems to occur in oxic surface waters just below the productive surface layer.[6,13] In the Arctic, additional sources of Hg and carbon are provided by sea-ice algae during spring blooms.[76] The presence of terrestrial organic matter and sea-ice layers that concentrates phytoplankton near the MeHg production zone may favor the Hg microbial methylation at shallow depths of the Arctic water column.[12,77] Shallower methylation occurring in Arctic waters may result in higher photochemical impact on MeHg before its assimilation in Arctic biota compared to North Atlantic marine food webs. This phenomenon could contribute to the higher feather Δ^{199}Hg values of FJL little auks compared to populations breeding at lower latitudes. The slight differences of Δ^{199}Hg values between northern and southern colonies of little auks are similar to the ranges recently observed in seabirds covering a wider latitudinal gradient (37−66°S) in the Southern Ocean, for which Δ^{199}Hg values increased from Antarctic (1.31−1.73‰) to subtropical (1.69−2.04‰) populations.[78] The slight variations of Δ^{199}Hg values also found between these distant sites of the Southern Ocean were translated into low differences of MeHg photochemical demethylation extents among sites and dominance of MeHg with a mesopelagic origin in these remote environments. As previously discussed, the vertical daily migration of copepods from deep water to the surface leads to the integration of Hg from relatively deep zones of the water column, therefore contributing to the incorporation of low photochemically impacted Hg in consumers.[75] Therefore, although the planktivorous little auks feed at surface waters on the photic zone, their relatively low feather Δ^{199}Hg values suggest that the Hg accumulated in their main prey could originate from Hg pools from deeper zones of the water column.

3.4. Spatial Correlation of Hg MIF Signatures and Carbon Stable Isotopes (δ^{13}C). The deposition of atmospheric Hg from mid-latitude anthropogenic emissions into the Arctic Ocean could contribute to the accumulation of MeHg from a distinct origin in Arctic-North Atlantic food

https://dx.doi.org/10.1021/acs.est.0c03285
Environ. Sci. Technol. XXXX, XXX, XXX−XXX

webs.[7] Although body feathers of little auk presented a relatively high range of Δ^{200}Hg signatures (from −0.23 to 0.17‰), the interpopulation differences were not significant (H = 3.685, p = 0.45) (Figure S5). No substantial interpopulation variations of Δ^{200}Hg values were observed for head feathers of little auks (−0.12‰ to 0.14‰); therefore, we cannot discriminate Hg sources from a distinct atmospheric origin among seabird wintering grounds. Nevertheless, the spatial trends of Δ^{200}Hg values observed in little auks are more variable than those previously reported in Arctic marine mammals and seabirds of Alaska (from −0.01 to 0.10‰; 71−54°N[79]) and in Antarctic and subtropical seabirds (from −0.02 to 0.04‰, 66−37°S[78]).

Large-scale ocean circulation and vertical transport processes throughout the water column could influence the distribution of distinct MeHg sources between the widely distributed compartments used by little auks. The exploration of carbon stable isotopes (δ^{13}C) of little auks could help in discriminating the potential contributions of distinct MeHg sources linked to the widely specific foraging habitats of little auks. Contrary to Hg isotopes, body feather δ^{13}C values do not reflect the period of summer but the molt period in late summer/early autumn (September) when they are grown.[45] To ensure only the integration of the summer, breeding period, we compared body feather Hg isotopes with blood δ^{13}C values. Little auks from FJL exhibited the lowest blood δ^{13}C values (−23.13 ± 0.84‰) and NW Greenland individuals showed the highest blood δ^{13}C values (−20.07 ± 0.35‰) relative to the rest of the colonies (H = 40.74, p < 0.0001) (Table S5). Head feather δ^{13}C values were used to distinguish little auk populations overwintering in western areas of the North Atlantic Ocean from those wintering in north-eastern areas (H = 26.28, p < 0.0001). The gradient of δ^{13}C values of head feathers increased from populations of FJL (−20.59 ± 0.40‰) and Bear Island (−20.35 ± 0.38‰) to Northwest (−19.41 ± 0.57‰) and East Greenland (−19.61 ± 0.46‰) populations. Latitudinal gradients of δ^{13}C values of the dissolved inorganic carbon are commonly observed in surface waters as an influence of the physical and biological processes.[71] For instance, it is known that CO_2 solubility is favored in cold oceanic waters and consequently, surface waters at high latitudes have relatively low δ^{13}C values due to the introduction of isotopically light atmospheric CO_2. By contrast, surface waters of outgassing upwelling equatorial areas have increased δ^{13}C values.[80,81] In parallel, the δ^{13}C values of primary producers are strongly influenced by the δ^{13}C values of dissolved inorganic carbon and, therefore, by the temperature gradients and CO_2 solubility.[71] Spatial gradients of sea surface temperature and CO_2 concentrations could thus explain the more depleted δ^{13}C baseline in cold high Arctic marine food webs and the enrichment in δ^{13}C values when going southward to North Atlantic oceanic areas. Furthermore, the dominance of distinct marine currents between the different wintering seabird sites could strongly determine the δ^{13}C at the base of the food webs. The FJL archipelago and surrounding high Arctic areas are strongly impacted by the Makarov and Arctic cold currents flowing southward from the north, and potentially contributing to transport isotopically depleted carbon from high-latitude areas. In contrast, little auk wintering regions near the Newfoundland Island (East and West Greenland populations) are affected by the Gulf Stream and North Atlantic Current,[45] which could supply carbon organic matter from warmer water masses.[82]

Significant negative linear relationships were obtained between Δ^{199}Hg and δ^{13}C values both in summer (R^2 = 0.17, p = 0.003) and in winter (R^2 = 0.31, p < 0.0001) (Figure 3). Interestingly, the negative relationship between Δ^{199}Hg and

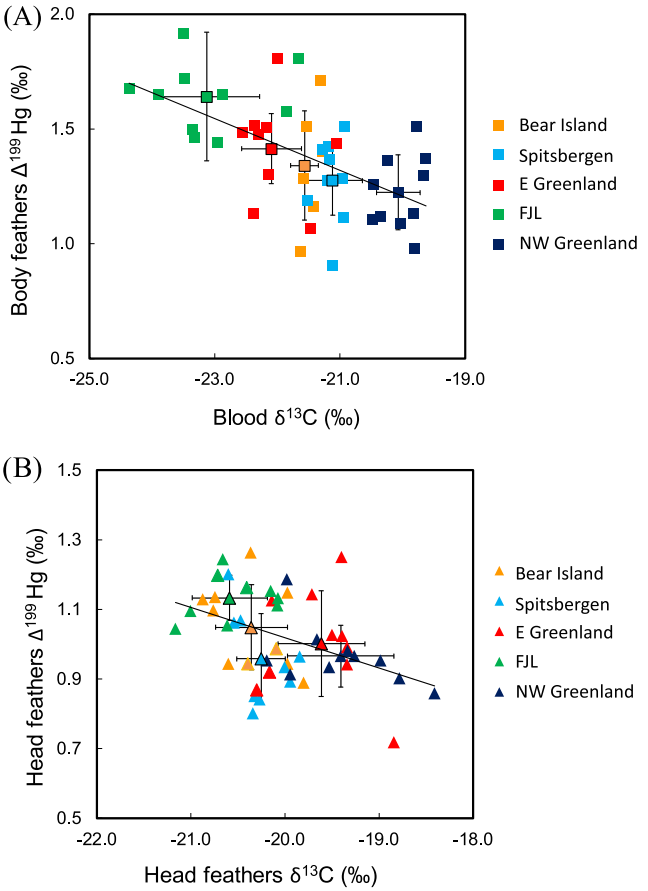

Figure 3. Carbon (δ^{13}C) vs MIF Hg signatures for (A) summer (body feathers) and (B) winter (head feathers) periods. Regression lines are (A) slope: −0.122 ± 0.026, intercept: −1.045 ± 0.558, R^2 = 0.31, p < 0.0001, and (B) slope: −0.088 ± 0.028, intercept: −0.746 ± 0.566, R^2 = 0.17, p = 0.003.

δ^{13}C values of little auks contrasts with those previously reported on eggs from guillemot species (or murres, *Uria aalge,* and *Uria lomvia*) breeding in the Alaskan Arctic.[26] These authors reported a co-enrichment of egg δ^{13}C and Δ^{199}Hg values linked to the transition from terrestrial to marine Hg sources and the subsequent reduction of Hg photochemistry in coastal reservoirs due to higher turbidity.[26] However, the wintering areas of little auks mainly correspond to more open oceanic areas as the study in the Bering Sea and probably do not present such a remarkable coastal−oceanic gradient. The significant correlation obtained here between Δ^{199}Hg and δ^{13}C signatures both in body and in head feathers of little auks reflects common spatial trends of summer and winter foraging grounds. This interesting relationship seems to be associated with both the spatial gradient of physical parameters controlling C isotopic baselines (temperature and CO_2 exchange in surface waters) and the extent of Hg photochemical processes. Probably, a higher stratification and impact of sea-ice cover in high Arctic oceanic zones favor the methylation of Hg in surface waters,[13] and the extent of photochemical reactions, leading to slightly positive Δ^{199}Hg

https://dx.doi.org/10.1021/acs.est.0c03285
Environ. Sci. Technol. XXXX, XXX, XXX−XXX

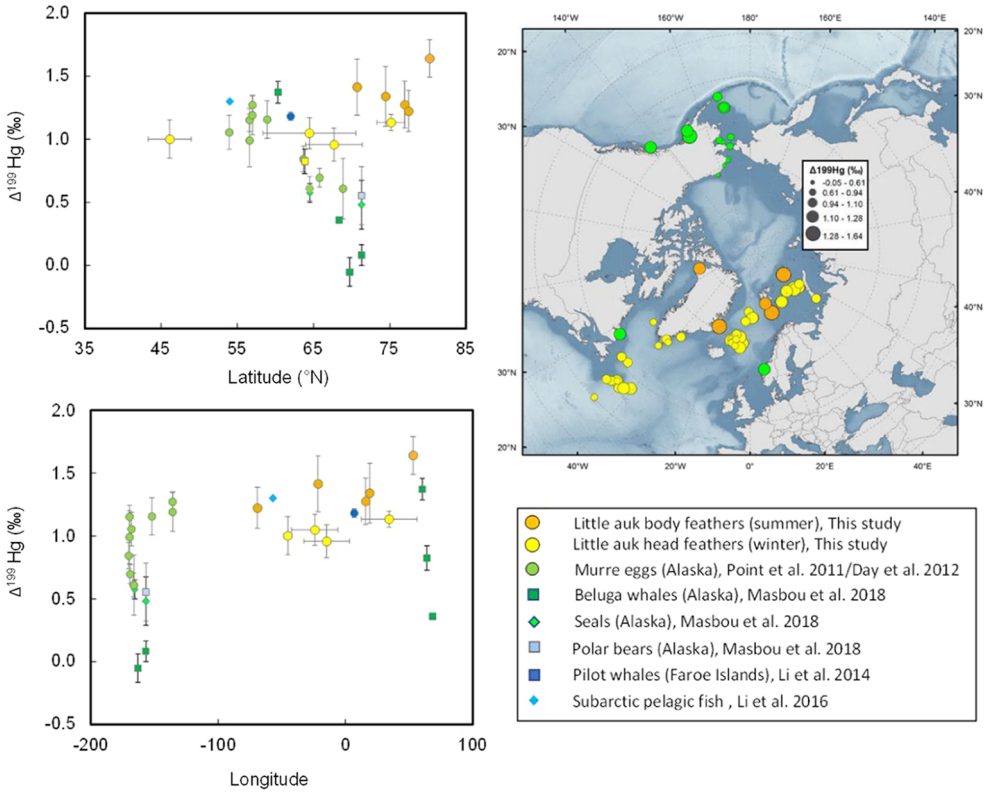

Figure 4. Compilation of Hg odd-MIF values (Δ^{199}Hg) of marine biota from spatially distant Arctic Regions. The map comprises both little auk breeding sites (orange), individual little auk median winter positions (yellow), and previously published data (green) including seabirds,[25,26] beluga whale, seals, and polar bears[79] from Alaskan Regions, pilot whales from the Faroe Islands,[28] and fish from the Labrador Sea.[83]

values and more negative δ^{13}C values of biota. The dominance of northern marine currents in this area would also contribute to depleted δ^{13}C values. Although we could consider the existence of distinct carbon inputs transported by the marine currents in these ecosystems (i.e., external carbon supply, planktonic production), the complex interaction of oceanographic and physical parameters governing these areas does not allow us to provide conclusive evidence from our data.

3.5. Geographically Distinct Hg Source Mixing Across the Arctic and North Atlantic Oceans. Our results suggest that the variations in relation to the longitude of the Hg concentrations, Δ^{199}Hg, and δ^{13}C values of little auks are linked to the assimilation of isotopically distinct MeHg depending on their wintering grounds. Figure 4 shows a compilation of Hg odd-MIF values observed in little auks compared to previous studies in Arctic biota over a wide spatial scale. The observed isotopic spatial variability across the different regions of the Arctic Ocean suggests the existence of two different Hg systems between East (Atlantic) and West (Pacific) Arctic Ocean regions. Our contrasting trend of Δ^{199}Hg from north to south population values relative to Western Arctic compartments[25,35] indicates that the presence of sea-ice cover is not the only driving factor controlling Hg photochemistry in the Eastern Arctic Ocean. Possibly, an additional supply of Hg and carbon sources by sea-ice algae may enhance the microbial/photochemical methylation and demethylation processes at shallower depths[6,13] in East Arctic regions, therefore contributing to the higher odd-MIF values of Hg accumulated in biota. The inversed relationship of Δ^{199}Hg and Δ^{200}Hg values of little auks with latitude is in contrast to the latitudinal covariation of Δ^{199}Hg and Δ^{200}Hg in biota from Western Arctic regions[79] and from Antarctic regions[78] and evidences a completely different functioning of Hg cycling compared to other polar marine environments. Complex Hg dynamics and ocean control factors seem to drive the increasing pattern of Hg isotopes from west to east regions of the Arctic Ocean. Future research assessing large-scale and long-term Hg contamination is necessary to have a complete understanding of the Hg exposure pathways and of the associated risks for the whole marine Arctic environment.

■ ASSOCIATED CONTENT

Supporting Information

The Supporting Information is available free of charge at https://pubs.acs.org/doi/10.1021/acs.est.0c03285.

Supplementary figures of feather Hg concentrations relative to Hg isotopic values of little auks, spatial trends of feather Hg MDF (δ^{202}Hg) and Hg even-MIF (Δ^{200}Hg) values; detailed QA/QC of total Hg concentrations, speciation and isotopic analyses; additional tables of the mean values of blood and feathers; details of statistical results; and supplementary discussion of the geographical Hg even-MIF trends of little auks (PDF)

■ AUTHOR INFORMATION

Corresponding Authors

Marina Renedo − *Littoral Environnement et Sociétés (LIENSs), UMR 7266 CNRS—La Rochelle Université, 17000 La Rochelle, France; Universite de Pau et des Pays de l'Adour, E2S UPPA, CNRS, IPREM, Institut des Sciences Analytiques et de Physico-chimie pour l'Environnement et les matériaux, 64000*

https://dx.doi.org/10.1021/acs.est.0c03285
Environ. Sci. Technol. XXXX, XXX, XXX−XXX

Pau, France; orcid.org/0000-0002-9224-8745; Email: marina.renedo@ird.fr

Jérôme Fort − *Littoral Environnement et Sociétés (LIENSs), UMR 7266 CNRS—La Rochelle Université, 17000 La Rochelle, France*; Email: jerome.fort@univ-lr.fr

Authors

David Amouroux − *Universite de Pau et des Pays de l'Adour, E2S UPPA, CNRS, IPREM, Institut des Sciences Analytiques et de Physico-chimie pour l'Environnement et les materiaux, 64000 Pau, France*

Céline Albert − *Littoral Environnement et Sociétés (LIENSs), UMR 7266 CNRS—La Rochelle Université, 17000 La Rochelle, France*

Sylvain Bérail − *Universite de Pau et des Pays de l'Adour, E2S UPPA, CNRS, IPREM, Institut des Sciences Analytiques et de Physico-chimie pour l'Environnement et les materiaux, 64000 Pau, France*

Vegard S. Bråthen − *Norwegian Institute for Nature Research, 7034 Trondheim, Norway*

Maria Gavrilo − *Association of Maritime Heritage: Sustain and Explore, 199106 Saint Petersburg, Russia*

David Grémillet − *Centre d'Etudes Biologiques de Chizé, UMR 7372 CNRS—La Rochelle Université, 79360 Villiers-en-Bois, France; Percy FitzPatrick Institute, DST/NRF Centre of Excellence, University of Cape Town, 7701 Cape Town, South Africa*

Hálfdán H. Helgason − *Norwegian Polar Institute, 9296 Tromsø, Norway*

Dariusz Jakubas − *Faculty of Biology, Gdańsk University, 80-308 Gdańsk, Poland*

Anders Mosbech − *Department of Bioscience, Aarhus University, 4000 Roskilde, Denmark*

Hallvard Strøm − *Norwegian Polar Institute, 9296 Tromsø, Norway*

Emmanuel Tessier − *Universite de Pau et des Pays de l'Adour, E2S UPPA, CNRS, IPREM, Institut des Sciences Analytiques et de Physico-chimie pour l'Environnement et les materiaux, 64000 Pau, France*

Katarzyna Wojczulanis-Jakubas − *Faculty of Biology, Gdańsk University, 80-308 Gdańsk, Poland*

Paco Bustamante − *Littoral Environnement et Sociétés (LIENSs), UMR 7266 CNRS—La Rochelle Université, 17000 La Rochelle, France; Institut Universitaire de France (IUF), 75005 Paris, France;* orcid.org/0000-0003-3877-9390

Complete contact information is available at: https://pubs.acs.org/10.1021/acs.est.0c03285

Notes

The authors declare no competing financial interest.

■ ACKNOWLEDGMENTS

The authors wish to thank the field workers who collected the samples. Field procedures were authorized by the Ethics Committee of Institut Polaire Français Paul Emile Victor (IPEV) and by the Comité de l'Environnement Polaire. This study received financial and logistical support from the French Agency for National Research (ANR MAMBA project ANR-16-TERC-0004, ILETOP project ANR-16-CE34-0005), the French Arctic Initiative—CNRS (PARCS project), the Mission pour l'Interdisciplinarité—CNRS (Changements en Sibérie project), and the French Polar Institute (IPEV−Pgr 388 ADACLIM). The IUF (Institut Universitaire de France) is also acknowledged for its support to P.B. as a senior member.

■ REFERENCES

(1) Tan, S. W.; Meiller, J. C.; Mahaffey, K. R. The Endocrine Effects of Mercury in Humans and Wildlife. *Crit. Rev. Toxicol.* **2009**, *39*, 228−269.

(2) Lehnherr, I.; St. Louis, V. L.; Hintelmann, H.; Kirk, J. L. Methylation of Inorganic Mercury in Polar Marine Waters. *Nat. Geosci.* **2011**, *4*, 298−302.

(3) Blum, J. D.; Popp, B. N.; Drazen, J. C.; Anela Choy, C.; Johnson, M. W. Methylmercury Production below the Mixed Layer in the North Pacific Ocean. *Nat. Geosci.* **2013**, *6*, 879−884.

(4) Mason, R. P.; Choi, A. L.; Fitzgerald, W. F.; Hammerschmidt, C. R.; Lamborg, C. H.; Soerensen, A. L.; Sunderland, E. M. Mercury Biogeochemical Cycling in the Ocean and Policy Implications. *Environ. Res.* **2012**, *119*, 101−117.

(5) Bowman, K. L.; Lamborg, C. H.; Agather, A. M. A Global Perspective on Mercury Cycling in the Ocean. *Sci. Total Environ.* **2020**, *710*, No. 136166.

(6) Soerensen, A. L.; Jacob, D. J.; Schartup, A. T.; Fisher, J. A.; Lehnherr, I.; Louis, V. L. S.; Heimbürger, L.; Sonke, J. E.; Krabbenhoft, D. P.; Sunderland, E. M. A Mass Budget for Mercury and Methylmercury in the Arctic Ocean. *Global Biogeochem. Cycles* **2016**, *30*, 560−575.

(7) Larose, C.; Dommergue, A.; Marusczak, N.; Coves, J.; Ferrari, C. P.; Schneider, D. Bioavailable Mercury Cycling in Polar Snowpacks. *Environ. Sci. Technol.* **2011**, *45*, 2150−2156.

(8) Beattie, S. A.; Armstrong, D.; Chaulk, A.; Comte, J.; Gosselin, M.; Wang, F. Total and Methylated Mercury in Arctic Multiyear Sea Ice. *Environ. Sci. Technol.* **2014**, *48*, 5575−5582.

(9) Sonke, J. E.; Teisserenc, R.; Heimbürger-Boavida, L.-E.; Petrova, M. V.; Marusczak, N.; Le Dantec, T.; Chupakov, A. V.; Li, C.; Thackray, C. P.; Sunderland, E. M.; Tananaev, N.; Pokrovsky, O. S. Eurasian River Spring Flood Observations Support Net Arctic Ocean Mercury Export to the Atmosphere and Atlantic Ocean. *Proc. Natl. Acad. Sci. U.S.A.* **2018**, *115*, E11586−E11594.

(10) Obrist, D.; Agnan, Y.; Jiskra, M.; Olson, C. L.; Dominique, P.; Hueber, J.; Moore, C. W.; Sonke, J.; Helmig, D. Tundra Uptake of Atmospheric Elemental Mercury Drives Arctic Mercury Pollution. *Nature* **2017**, *547*, 201−204.

(11) Kirk, J. L.; St. Louis, V. L.; Hintelmann, H.; Lehnherr, I.; Else, B.; Poissant, L. Methylated Mercury Species in Marine Waters of the Canadian High and Sub Arctic. *Environ. Sci. Technol.* **2008**, *42*, 8367−8373.

(12) Gionfriddo, C. M.; Tate, M. T.; Wick, R. R.; Schultz, M. B.; Zemla, A.; Thelen, M. P.; Schofield, R.; Krabbenhoft, D. P.; Holt, K. E.; Moreau, J. W. Microbial Mercury Methylation in Antarctic Sea Ice. *Nat. Microbiol.* **2016**, *1*, No. 16127.

(13) Heimbürger, L. E.; Sonke, J. E.; Cossa, D.; Point, D.; Lagane, C.; Laffont, L.; Galfond, B. T.; Nicolaus, M.; Rabe, B.; van der Loeff, M. R. Shallow Methylmercury Production in the Marginal Sea Ice Zone of the Central Arctic Ocean. *Sci. Rep.* **2015**, *5*, No. 10318.

(14) Villar, E.; Cabrol, L.; Heimbürger-Boavida, L. E. Widespread Microbial Mercury Methylation Genes in the Global Ocean. *Environ. Microbiol. Rep.* **2020**, *12*, 277−287.

(15) AMAP. *Arctic Monitoring and Assessment Program 2011: Mercury in the Arctic*; Oslo, 2011.

(16) AMAP. *AMAP Assessment 2018: Biological Effects of Contaminants on Arctic Wildlife and Fish*; Oslo, 2018.

(17) Thompson, D. R.; Furness, R. W.; Walsh, P. M. Historical Changes in Mercury Concentrations in the Marine Ecosystem of the North and North-East Atlantic Ocean as Indicated by Seabird Feathers. *J. Appl. Ecol.* **1992**, *29*, 79−84.

(18) Carravieri, A.; Cherel, Y.; Jaeger, A.; Churlaud, C.; Bustamante, P. Penguins as Bioindicators of Mercury Contamination in the Southern Indian Ocean: Geographical and Temporal Trends. *Environ. Pollut.* **2016**, *213*, 195−205.

https://dx.doi.org/10.1021/acs.est.0c03285
Environ. Sci. Technol. XXXX, XXX, XXX−XXX

(19) Rigét, F.; Braune, B.; Bignert, A.; Wilson, S.; Aars, J.; Born, E.; Dam, M.; Dietz, R.; Evans, M.; Evans, T.; Gamberg, M.; Gantner, N.; Green, N.; Gunnlaugsdóttir, H.; Kannan, K.; Letcher, R.; Muir, D.; Roach, P.; Sonne, C.; Stern, G.; Wiig, O. Temporal Trends of Hg in Arctic Biota, an Update. *Sci. Total Environ.* **2011**, *409*, 3520−3526.
(20) Dietz, R.; Sonne, C.; Basu, N.; Braune, B.; O'Hara, T.; Letcher, R. J.; Scheuhammer, T.; Andersen, M.; Andreasen, C.; Andriashek, D.; Asmund, G.; Aubail, A.; Baagøe, H.; Born, E. W.; Chan, H. M.; Derocher, A. E.; Grandjean, P.; Knott, K.; Kirkegaard, M.; Krey, A.; Lunn, N.; Messier, F.; Obbard, M.; Olsen, M. T.; Ostertag, S.; Peacock, E.; Renzoni, A.; Rigét, F. F.; Skaare, J. U.; Stern, G.; Stirling, I.; Taylor, M.; Wiig, Ø.; Wilson, S.; Aars, J. What Are the Toxicological Effects of Mercury in Arctic Biota? *Sci. Total Environ.* **2013**, *443*, 775−790.
(21) Albert, C.; Renedo, M.; Bustamante, P.; Fort, J. Using Blood and Feathers to Investigate Large-Scale Hg Contamination in Arctic Seabirds: A Review. *Environ. Res.* **2019**, *177*, No. 108588.
(22) Fort, J.; Robertson, G. J.; Grémillet, D.; Traisnel, G.; Bustamante, P. Spatial Ecotoxicology: Migratory Arctic Seabirds Are Exposed to Mercury Contamination While Overwintering in the Northwest Atlantic. *Environ. Sci. Technol.* **2014**, *48*, 11560−11567.
(23) Fleishman, A. B.; Orben, R. A.; Kokubun, N.; Will, A.; Paredes, R.; Ackerman, J. T.; Takahashi, A.; Kitaysky, A. S.; Shaffer, S. A. Wintering in the Western Subarctic Pacific Increases Mercury Contamination of Red-Legged Kittiwakes. *Environ. Sci. Technol.* **2019**, *53*, 13398−13407.
(24) Renedo, M.; Amouroux, D.; Pedrero, Z.; Bustamante, P.; Cherel, Y. Identification of Sources and Bioaccumulation Pathways of MeHg in Subantarctic Penguins: A Stable Isotopic Investigation. *Sci. Rep.* **2018**, *8*, No. 8865.
(25) Point, D.; Sonke, J. E.; Day, R. D.; Roseneau, D. G.; Hobson, K. A.; Vander Pol, S. S.; Moors, A. J.; Pugh, R. S.; Donard, O. F. X.; Becker, P. R. Methylmercury Photodegradation Influenced by Sea-Ice Cover in Arctic Marine Ecosystems. *Nat. Geosci.* **2011**, *4*, 188−194.
(26) Day, R. D.; Roseneau, D. G.; Berail, S.; Hobson, K. A.; Donard, O. F. X.; Vander Pol, S. S.; Pugh, R. S.; Moors, A. J.; Long, S. E.; Becker, P. R. Mercury Stable Isotopes in Seabird Eggs Reflect a Gradient from Terrestrial Geogenic to Oceanic Mercury Reservoirs. *Environ. Sci. Technol.* **2012**, *46*, 5327−5335.
(27) Blum, J. D.; Sherman, L. S.; Johnson, M. W. Mercury Isotopes in Earth and Environmental Sciences. *Annu. Rev. Earth Planet. Sci.* **2014**, *42*, 249−269.
(28) Li, M.; Sherman, L. S.; Blum, J. D.; Grandjean, P.; Mikkelsen, B.; Weihe, P.; Sunderland, E. M.; Shine, J. P. Assessing Sources of Human Methylmercury Exposure Using Stable Mercury Isotopes. *Environ. Sci. Technol.* **2014**, *48*, 8800−8806.
(29) Cransveld, A.; Amouroux, D.; Tessier, E.; Koutrakis, E.; Ozturk, A. A.; Bettoso, N.; Mieiro, C. L.; Berail, S.; Barre, J. P. G.; Sturaro, N.; Schnitzler, J. G.; Das, K. Mercury Stable Isotopes Discriminate Different Populations of European Seabass and Trace Potential Hg Sources around Europe. *Environ. Sci. Technol.* **2017**, *51*, 12219−12228.
(30) Kritee, K.; Barkay, T.; Blum, J. D. Mass Dependent Stable Isotope Fractionation of Mercury during Mer Mediated Microbial Degradation of Monomethylmercury. *Geochim. Cosmochim. Acta* **2009**, *73*, 1285−1296.
(31) Kritee, K.; Blum, J. D.; Barkay, T. Mercury Stable Isotope Fractionation during Reduction of Hg(II) by Different Microbial Pathways. *Environ. Sci. Technol.* **2008**, *42*, 9171−9177.
(32) Zheng, W.; Foucher, D.; Hintelmann, H. Mercury Isotope Fractionation during Volatilization of Hg(0) from Solution into the Gas Phase. *J. Anal. At. Spectrom.* **2007**, *22*, 1097−1104.
(33) Kwon, S. Y.; Blum, J. D.; Chirby, M. A.; Chesney, E. J. Application of Mercury Isotopes for Tracing Trophic Transfer and Internal Distribution of Mercury in Marine Fish Feeding Experiments. *Environ. Toxicol. Chem.* **2013**, *32*, 2322−2330.
(34) Kwon, S. Y.; Blum, J. D.; Carvan, M. J.; Basu, N.; Head, J. A.; Madenjian, C. P.; David, S. R. Absence of Fractionation of Mercury Isotopes during Trophic Transfer of Methylmercury to Freshwater Fish in Captivity. *Environ. Sci. Technol.* **2012**, *46*, 7527−7534.
(35) Masbou, J.; Point, D.; Sonke, J. E.; Frappart, F.; Perrot, V.; Amouroux, D.; Richard, P.; Becker, P. R. Hg Stable Isotope Time Trend in Ringed Seals Registers Decreasing Sea Ice Cover in the Alaskan Arctic. *Environ. Sci. Technol.* **2015**, *49*, 8977−8985.
(36) Chen, J.; Hintelmann, H.; Feng, X.; Dimock, B. Unusual Fractionation of Both Odd and Even Mercury Isotopes in Precipitation from Peterborough, ON, Canada. *Geochim. Cosmochim. Acta* **2012**, *90*, 33−46.
(37) Gratz, L. E.; Keeler, G. J.; Blum, J. D.; Sherman, L. S. Isotopic Composition and Fractionation of Mercury in Great Lakes Precipitation and Ambient Air. *Environ. Sci. Technol.* **2010**, *44*, 7764−7770.
(38) Sherman, L. S.; Blum, J. D.; Douglas, T. A.; Steffen, A. Frost Flowers Growing in the Arctic Ocean-Atmosphere-Sea Ice-Snow Interface: 2. Mercury Exchange between the Atmosphere, Snow, and Frost Flowers. *J. Geophys. Res.* **2012**, *117*, 1−10.
(39) Demers, J. D.; Blum, J. D.; Zak, D. R. Mercury Isotopes in a Forested Ecosystem: Implications for Air-Surface Exchange Dynamics and the Global Mercury Cycle. *Global Biogeochem. Cycles* **2013**, *27*, 222−238.
(40) Enrico, M.; Roux, G. L.; Marusczak, N.; Heimbürger, L. E.; Claustres, A.; Fu, X.; Sun, R.; Sonke, J. E. Atmospheric Mercury Transfer to Peat Bogs Dominated by Gaseous Elemental Mercury Dry Deposition. *Environ. Sci. Technol.* **2016**, *50*, 2405−2412.
(41) Keslinka, L. K.; Wojczulanis-Jakubas, K.; Jakubas, D.; Neubauer, G. Determinants of the Little Auk (Alle Alle) Breeding Colony Location and Size in W and NW Coast of Spitsbergen. *PLoS One* **2019**, *14*, No. e0212668.
(42) Kovacs, K. M.; Lydersen, C. *Birds and Mammals of Svalbard*; Norwegian Polar Institute: Tromsø, 2006.
(43) Harding, A. M. A.; Hobson, K. A.; Walkusz, W.; Dmoch, K.; Karnovsky, N. J.; Van Pelt, T. I.; Lifjeld, J. T. Can Stable Isotope (Δ13C and Δ15N) Measurements of Little Auk (Alle Alle) Adults and Chicks Be Used to Track Changes in High-Arctic Marine Foodwebs? *Polar Biol.* **2008**, *31*, 725−733.
(44) Grémillet, D.; Welcker, J.; Karnovsky, N. J.; Walkusz, W.; Hall, M. E.; Fort, J.; Brown, Z. W.; Speakman, J. R.; Harding, A. M. A. Little Auks Buffer the Impact of Current Arctic Climate Change. *Mar. Ecol.: Prog. Ser.* **2012**, *454*, 197−206.
(45) Fort, J.; Moe, B.; Strøm, H.; Grémillet, D.; Welcker, J.; Schultner, J.; Jerstad, K.; Johansen, K. L.; Phillips, R. A.; Mosbech, A. Multicolony Tracking Reveals Potential Threats to Little Auks Wintering in the North Atlantic from Marine Pollution and Shrinking Sea Ice Cover. *Diversity Distrib.* **2013**, *19*, 1322−1332.
(46) Fort, J.; Gremillet, D.; Traisnel, G.; Amelineau, F.; Bustamante, P. Does Temporal Variation of Mercury Levels in Arctic Seabirds Reflect Changes in Global Environmental Contamination, or a Modification of Arctic Marine Food Web Functioning? *Environ. Pollut.* **2016**, *211*, 382−388.
(47) Furness, R. W.; Muirhead, S. J.; Woodburn, M. Using Bird Feathers to Measure Mercury in the Environment: Relationships between Mercury Content and Moult. *Mar. Pollut. Bull.* **1986**, *17*, 27−30.
(48) Honda, K.; Nasu, T.; Tatsukawa, R. Seasonal Changes in Mercury Accumulation in the Black-Eared Kite *Milvus migrans lineatus*. *Environ. Pollut., Ser. A* **1986**, *42*, 325−334.
(49) Hobson, K. A.; Clark, R. G. Assessing Avian Diets Using Stable Isotopes I: Turnover of ^{13}C in Tissues. *Condor* **1992**, *94*, 181−188.
(50) Bearhop, S.; Waldron, S.; Votier, S. C.; Furness, R. W. Factors That Influence Assimilation Rates and Fractionation of Nitrogen and Carbon Stable Isotopes in Avian Blood and Feathers. *Physiol. Biochem. Zool.* **2002**, *75*, 451−458.
(51) Fort, J.; Beaugrand, G.; Grémillet, D.; Phillips, R. A. Biologging, Remotely-Sensed Oceanography and the Continuous Plankton Recorder Reveal the Environmental Determinants of a Seabird Wintering Hotspot. *PLoS One* **2012**, *7*, No. e41194.

https://dx.doi.org/10.1021/acs.est.0c03285
Environ. Sci. Technol. XXXX, XXX, XXX−XXX

(52) Grissot, A.; Graham, I. M.; Quinn, L.; Bråthen, V. S.; Thompson, P. M. Breeding Status Influences Timing but Not Duration of Moult in the Northern Fulmar *Fulmarus glacialis*. *Ibis* **2020**, *162*, 446−459.
(53) Carravieri, A.; Bustamante, P.; Churlaud, C.; Fromant, A.; Cherel, Y. Moulting Patterns Drive Within-Individual Variations of Stable Isotopes and Mercury in Seabird Body Feathers: Implications for Monitoring of the Marine Environment. *Mar. Biol.* **2014**, *161*, 963−968.
(54) Peterson, S. H.; Ackerman, J. T.; Toney, M.; Herzog, M. P. Mercury Concentrations Vary Within and Among Individual Bird Feathers: A Critical Evaluation and Guidelines for Feather Use in Mercury Monitoring Programs. *Environ. Toxicol. Chem.* **2019**, *38*, 1164−1187.
(55) Renedo, M.; Bustamante, P.; Tessier, E.; Pedrero, Z.; Cherel, Y.; Amouroux, D. Assessment of Mercury Speciation in Feathers Using Species-Specific Isotope Dilution Analysis. *Talanta* **2017**, *174*, 100−110.
(56) Renedo, M.; Amouroux, D.; Duval, B.; Carravieri, A.; Tessier, E.; Barre, J.; Bérail, S.; Pedrero, Z.; Cherel, Y.; Bustamante, P. Seabird Tissues As Efficient Biomonitoring Tools for Hg Isotopic Investigations: Implications of Using Blood and Feathers from Chicks and Adults. *Environ. Sci. Technol.* **2018**, *52*, 4227−4234.
(57) Yamakawa, A.; Takeuchi, A.; Shibata, Y.; Berail, S.; Donard, O. F. X. Determination of Hg Isotopic Compositions in Certified Reference Material NIES No. 13 Human Hair by Cold Vapor Generation Multi-Collector Inductively Coupled Plasma Mass Spectrometry. *Accredit. Qual. Assur.* **2016**, *21*, 197−202.
(58) R Core Team. *A Language and Environment for Statistical Computing*; R Foundation for Statistical Computing: Vienna, Austria, 2016.
(59) Bates, D.; Mächler, M.; Bolker, B. M.; Walker, S. C. Fitting Linear Mixed-Effects Models Using Lme4 *J. Stat. Software* 2015, *671* DOI: 10.18637/jss.v067.i01.
(60) Salmerón, R.; García, C. B.; García, J. Variance Inflation Factor and Condition Number in Multiple Linear Regression. *J. Stat. Computation Simul.* **2018**, *88*, 2365−2384.
(61) Zuur, A. F.; Ieno, E. N.; Walker, N. J.; Saveliev, A. A.; Smith, G. M. Mixed Effects Models and Extensions in Ecology with R. *J. Stat. Software* **2009**, *32*, 1−4.
(62) Meredith, M. M. *Package ' Wiqid'*, 2020.
(63) Jaeger, B. C. *Computes R Squared for Mixed (Multilevel) Model Packag. 'r2glmm' 2017*, 12, 2017.
(64) Davis, W. C.; Vander Pol, S. S.; Schantz, M. M.; Long, S. E.; Day, R. D.; Christopher, S. J. An Accurate and Sensitive Method for the Determination of Methylmercury in Biological Specimens Using GC-ICP-MS with Solid Phase Microextraction. *J. Anal. At. Spectrom.* **2004**, *19*, 1546−1551.
(65) Bond, A. L.; Diamond, A. W. Total and Methyl Mercury Concentrations in Seabird Feathers and Eggs. *Arch. Environ. Contam. Toxicol.* **2009**, *56*, 286−291.
(66) Rosing-Asvid, A.; Hedeholm, R.; Arendt, K. E.; Fort, J.; Robertson, G. J. Winter Diet of the Little Auk (Alle Alle) in the Northwest Atlantic. *Polar Biol.* **2013**, *36*, 1601−1608.
(67) Fort, J.; Cherel, Y.; Harding, A. M. A.; Welcker, J.; Jakubas, D.; Steen, H.; Karnovsky, N. J.; Grémillet, D. Geographic and Seasonal Variability in the Isotopic Niche of Little Auks. *Mar. Ecol.: Prog. Ser.* **2010**, *414*, 293−302.
(68) Welcker, J.; Harding, A. M. A.; Karnovsky, N. J.; Steen, H.; Strøm, H.; Gabrielsen, G. W. Flexibility in the Bimodal Foraging Strategy of a High Arctic Alcid, the Little Auk Alle Alle. *J. Avian Biol.* **2009**, *40*, 388−399.
(69) Hobson, K. A.; Clark, R. G. Assessing Avian Diets Using Stable Isotopes II: Factors Influencing Diet-Tissue Fractionation. *Condor* **1992**, *94*, 189−197.
(70) Graham, B. S.; Koch, P. L.; Newsome, S. D.; McMahon, K. W.; Aurioles, D. Using Isoscapes to Trace the Movements and Foraging Behavior of Top Predators in Oceanic Ecosystems. In *Isoscapes: Understanding Movement, Pattern, and Process on Earth Through Isotope Mapping*; Springer: Dordrecht, 2010; pp 299−318.
(71) McMahon, K. W.; Hamady, L. L.; Thorrold, S. R. A Review of Ecogeochemistry Approaches to Estimating Movements of Marine Animals. *Limnol. Oceanogr.* **2013**, *58*, 697−714.
(72) Kürten, B.; Painting, S. J.; Struck, U.; Polunin, N. V. C.; Middelburg, J. J. Tracking Seasonal Changes in North Sea Zooplankton Trophic Dynamics Using Stable Isotopes. *Biogeochemistry* **2013**, *113*, 167−187.
(73) Renedo, M.; Pedrero, Z.; Amouroux, D.; Cherel, Y.; Bustamante, P. Mercury Isotopes of Key Tissues Document Mercury Metabolic Processes in Seabirds. *Chemosphere* **2021**, *263*, No. 127777.
(74) Stempniewicz, L.; Skakuj, M.; Iliszko, L. The Little Auk Alle Alle Polaris of Franz Josef Land: A Comparison with Svalbard Alle A. alle Populations. *Polar Res.* **1996**, *15*, 1−10.
(75) Motta, L. C.; Blum, J. D.; Johnson, M. W.; Umhau, B. P.; Popp, B. N.; Washburn, S. J.; Drazen, J. C.; Benitez-Nelson, C. R.; Hannides, C. C. S.; Close, H. G.; Lamborg, C. H. Mercury Cycling in the North Pacific Subtropical Gyre as Revealed by Mercury Stable Isotope Ratios. *Global Biogeochem. Cycles* **2019**, *33*, 777−794.
(76) Burt, A.; Wang, F.; Pučko, M.; Mundy, C. J.; Gosselin, M.; Philippe, B.; Poulin, M.; Tremblay, J. É.; Stern, G. A. Mercury Uptake within an Ice Algal Community during the Spring Bloom in First-Year Arctic Sea Ice. *J. Geophys. Res.: Oceans* **2013**, *118*, 4746−4754.
(77) Schartup, A. T.; Balcom, P. H.; Soerensen, A. L.; Gosnell, K. J.; Calder, R. S. D.; Mason, R. P.; Sunderland, E. M. Freshwater Discharges Drive High Levels of Methylmercury in Arctic Marine Biota. *Proc. Natl. Acad. Sci. U.S.A.* **2015**, *112*, 11789−11794.
(78) Renedo, M.; Bustamante, P.; Cherel, Y.; Pedrero, Z.; Tessier, E.; Amouroux, D. A "Seabird-Eye" on Mercury Stable Isotopes and Cycling in the Southern Ocean. *Sci. Total Environ.* **2020**, *742*, No. 140499.
(79) Masbou, J.; Sonke, J. E.; Amouroux, D.; Guillou, G.; Becker, P. R.; Point, D. Hg-Stable Isotope Variations in Marine Top Predators of the Western Arctic Ocean. *ACS Earth Space Chem.* **2018**, *2*, 479−490.
(80) Lynch-Stieglitz, J.; Stocker, T. F.; Broecker, W. S.; Fairbanks, R. G. The Influence of Air-sea Exchange on the Isotopic Composition of Oceanic Carbon: Observations and Modeling. *Global Biogeochem. Cycles* **1995**, *9*, 653−665.
(81) Gruber, N.; Keeling, D.; Bacastow, R. B.; Guenther, P. R.; Lueker, T. J.; Wahlen, M.; Meijer, H. A. J.; Mook, W. G.; Stocker, T. F. Spatiotemporal Patterns of Carbon-13 in the Global Surface Oceans and the Oceanic Suess Effect. *Global Biogeochem. Cycles* **1999**, *13*, 307−335.
(82) Fontela, M.; García-Ibáñez, M. I.; Hansell, D. A.; Mercier, H.; Pérez, F. F. Dissolved Organic Carbon in the North Atlantic Meridional Overturning Circulation. *Sci. Rep.* **2016**, *6*, No. 26931.
(83) Li, M.; Schartup, A. T.; Valberg, A. P.; Ewald, J. D.; David, P.; Yin, R.; Balcom, P. H.; Sunderland, E. M. Environmental Origins of Methylmercury Accumulated in Subarctic Estuarine Fish Indicated by Mercury Stable Isotopes. *Environ. Sci. Technol.* **2016**, *50*, 11559−15568.

https://dx.doi.org/10.1021/acs.est.0c03285
Environ. Sci. Technol. XXXX, XXX, XXX−XXX